

Meshfree Inelastic Frame Analysis

Theory & Results

Louie L. Yaw, Sashi Kunnath and N. Sukumar

University of California, Davis
Department of Civil and Environmental Engineering

Minisymposium 47 – Recent Advances in Modeling of
Engineering Materials/Systems
USNCCM9 – San Francisco
July 24, 2007



Acknowledgements

- Funding provided by Walla Walla College
- N. Sukumar acknowledges research support of NSF (Grant CMMI-0626481)
- Helpful discussions with Dr. Michael Puso, Lawrence Livermore National Laboratory
- Helpful discussions with Professor Boris Jeremic, UC Davis



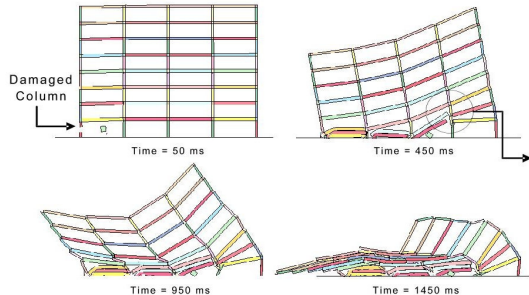
Outline

- 1 Motivation
- 2 Coupled finite element and meshfree method
 - Formulation
 - Numerical implementation
- 3 Application to wide-flange steel sections
- 4 Validation of methodology
 - Linear elastic cantilever I-beam
 - Inelastic Problems
- 5 Conclusions



Motivation

- Goal to advance collapse simulation technology
- Current FE technology unsatisfactory for large deformations at collapse limit states
- To explore feasibility of meshfree approach



Outline

- 1 Motivation
- 2 Coupled finite element and meshfree method
 - Formulation
 - Numerical implementation
- 3 Application to wide-flange steel sections
- 4 Validation of methodology
 - Linear elastic cantilever I-beam
 - Inelastic Problems
- 5 Conclusions



MLS Shape Functions Derivation

- Start with displacement approximation

$$\mathbf{u}^h(\mathbf{x}) = \sum_{a=1}^n \phi_a(\mathbf{x}) \mathbf{d}_a \equiv \boldsymbol{\phi}^T \mathbf{d}$$

- Shape function ϕ_a is of the form (Belytschko et al 1996)

$$\phi_a(\mathbf{x}) = \mathbf{P}^T(\mathbf{x}_a) \boldsymbol{\alpha}(\mathbf{x}) w(\mathbf{x}_a),$$

where $\mathbf{P}(\mathbf{x}) = \{1 \ x \ y\}^T$ is a linear basis in two dimensions, $\boldsymbol{\alpha}(\mathbf{x})$ is a vector of unknowns to be determined and $w(\mathbf{x}) \geq 0$ is a weighting function



MLS Shape Functions Derivation

- The ϕ 's must satisfy *reproducing conditions*

$$\mathbf{P}(\mathbf{x}) = \sum_{a=1}^n \mathbf{P}(\mathbf{x}_a) \phi_a(\mathbf{x})$$

- Substitution of ϕ_a into $\mathbf{P}(\mathbf{x})$ and solving for α yields

$$\alpha(\mathbf{x}) = \mathbf{A}^{-1}(\mathbf{x}) \mathbf{P}(\mathbf{x})$$

- Finally, substituting α into ϕ_a gives

$$\phi_a(\mathbf{x}) = \mathbf{P}^T(\mathbf{x}_a) \mathbf{A}^{-1}(\mathbf{x}) \mathbf{P}(\mathbf{x}) w(\mathbf{x}_a),$$

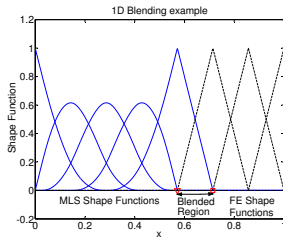
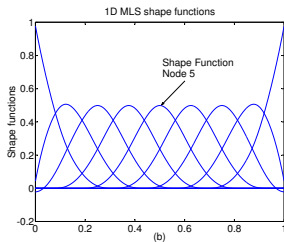
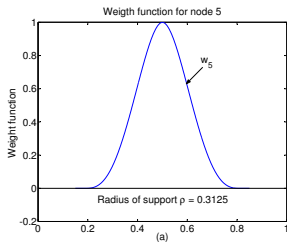
where $\mathbf{A} = \sum_{a=1}^n \mathbf{P}(\mathbf{x}_a) \mathbf{P}^T(\mathbf{x}_a) w(\mathbf{x}_a)$



Enforcing boundary conditions

- MLS (meshfree) shape functions do not have the Kronecker-delta property
- Hence MLS shape functions are blended with quadrilateral FE shape functions at essential B.C.'s
- Then essential boundary conditions are enforced on the finite element nodes in the standard way
- The blending technique proposed by Huerta and Fernández-Méndez (2004) is adopted





Nodal Integration

- *Smoothed* strain tensor for node a (per Chen et al (2001))

$$\varepsilon_{ij}(\mathbf{x}_a) = \frac{1}{2A_a} \int_{V_a} (u_{i,j} + u_{j,i}) dV = \frac{1}{2A_a} \int_{S_a} (u_i n_j + u_j n_i) dS$$

- Strain-displacement relation

$$\boldsymbol{\varepsilon}(\mathbf{x}_a) = \sum_{b=1}^6 \mathbf{B}_b(\mathbf{x}_a) \mathbf{d}_b \equiv \mathbf{Bd}$$



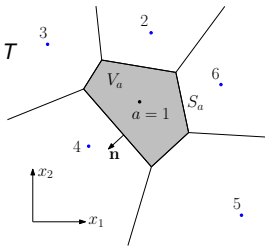
Nodal Integration

- Strain-displacement definitions

$$\boldsymbol{\varepsilon} = [\varepsilon_{11} \ \varepsilon_{22} \ 2\varepsilon_{12}]^T \quad \text{and} \quad \mathbf{d}_a = [d_{a1} \ d_{a2}]^T$$

$$\mathbf{B}_b(\mathbf{x}_a) = \begin{bmatrix} b_{b1}(\mathbf{x}_a) & 0 \\ 0 & b_{b2}(\mathbf{x}_a) \\ b_{b2}(\mathbf{x}_a) & b_{b1}(\mathbf{x}_a) \end{bmatrix}$$

$$b_{bi}(\mathbf{x}_a) = \frac{1}{A_a} \int_{S_a} \phi_b(\mathbf{x}) n_i(\mathbf{x}) dS$$



- Nodally integrated stiffness matrix

$$\mathbf{K}_{bc} = \sum_{a=1}^n \mathbf{B}_b^T(\mathbf{x}_a) \mathbf{C} \mathbf{B}_c(\mathbf{x}_a) A_{at}$$



Outline

- 1 Motivation
- 2 Coupled finite element and meshfree method
 - Formulation
 - Numerical implementation
- 3 Application to wide-flange steel sections
- 4 Validation of methodology
 - Linear elastic cantilever I-beam
 - Inelastic Problems
- 5 Conclusions



Stabilization of Nodal Integration

- Nodal integration w/o stabilization leads to
 - a. hourglass modes
 - b. spurious low energy modes
 - c. and locking
- Following Puso and Solberg (2006) stabilization is provided to the stiffness matrix as follows:

$$\mathbf{K}^S = (1 - \alpha_S)\mathbf{K}^{MLS} + \alpha_S\mathbf{K}^{FE},$$

where \mathbf{K}^S is the stabilized matrix and $\alpha_S = 0.05$ is called the stabilization factor



Nonlinear analysis

- Loads applied incrementally
- At global level a Newton-Raphson scheme is used to iterate the linearized system of equations until equilibrium is achieved

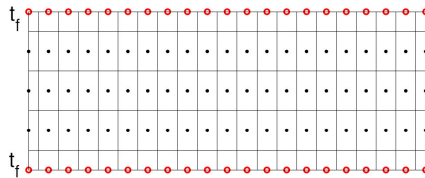
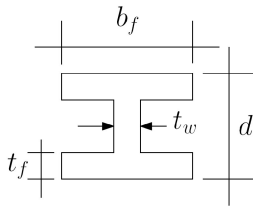
$$\mathbf{K}_{n+1}^{t(\nu)} \Delta \mathbf{d}_n^{(\nu)} = \mathbf{f}_{n+1}^{ext} - \mathbf{f}_{n+1}^{int(\nu)}$$

- At the constitutive level for $J2$ plasticity a radial return scheme is used (Simo and Hughes (1998))



Meshfree analysis of wide-flange steel sections

- Based on the meshfree nodal discretization of a beam a Voronoi diagram is generated.
- A thickness is specified for each Voronoi cell.
- To get wide-flange behavior a web thickness and a flange thickness is specified.



- Flange thickness b_f specified
- Web thickness t_w specified



Outline

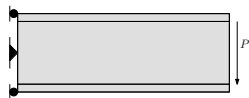
- 1 Motivation
- 2 Coupled finite element and meshfree method
 - Formulation
 - Numerical implementation
- 3 Application to wide-flange steel sections
- 4 Validation of methodology**
 - Linear elastic cantilever I-beam**
 - Inelastic Problems
- 5 Conclusions



Linear elastic cantilever I-beam

Results for normalized tip displacement and maximum bending stress, where $\delta_{theor.} = 0.0308$ in and $\sigma_{theor.} = 25.0$ ksi.

Grid	$\delta/\delta_{theor.}$ (in)	$\sigma_{xx}/\sigma_{theor.}$ (ksi)
11 × 3	1.045	0.77
21 × 5	1.025	0.89
31 × 7	1.016	0.94
41 × 9	1.012	0.95
51 × 11	1.010	0.96
61 × 13	1.009	0.97



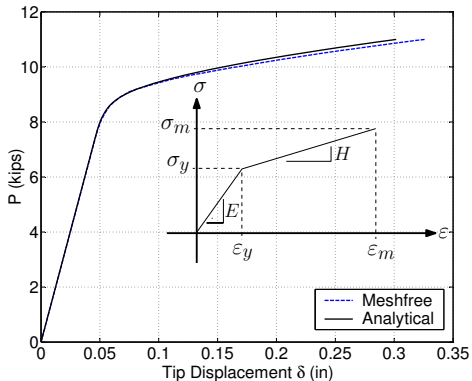
Outline

- 1 Motivation
- 2 Coupled finite element and meshfree method
 - Formulation
 - Numerical implementation
- 3 Application to wide-flange steel sections
- 4 Validation of methodology
 - Linear elastic cantilever I-beam
 - Inelastic Problems
- 5 Conclusions

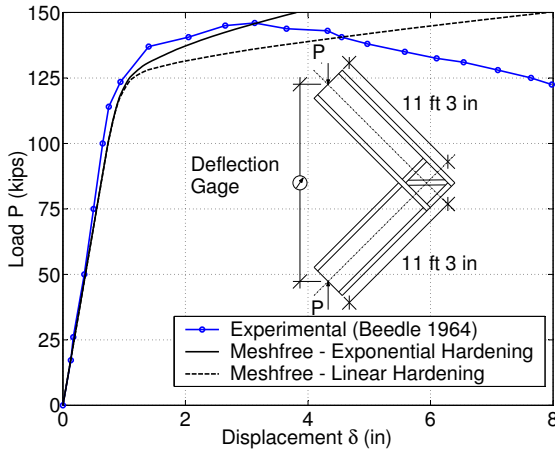


Elasto-plastic cantilever I-beam

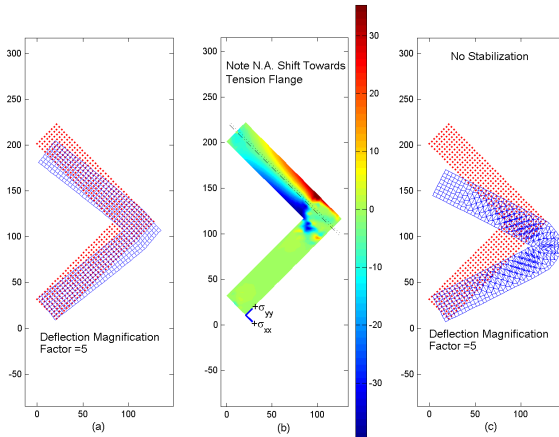
J2 plasticity with linear hardening



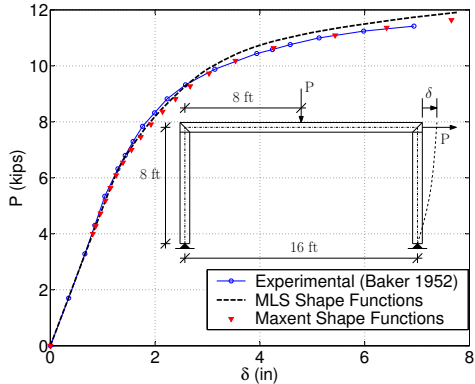
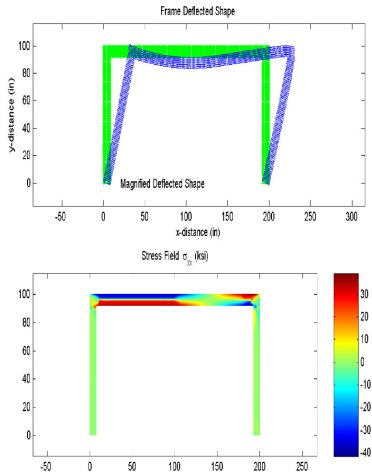
Frame corner connection: Load deflection response



Frame corner connection: Displacement and stress



Inelastic frame analysis



Conclusions

- Demonstrated feasibility of wide-flange beam analysis under plane stress
- A coupled FE and meshfree method shows promise for inelastic frame analysis
- Demonstrated success of Maxent shape functions
- Further research is ongoing to extend this for large deformations to enable collapse simulations.

